Assessment of KAERI Bundle CHF Database for Design Applications of Soluble Boron-free Small Modular Reactors

Juhyung Lee*, Seong-Jin Kim, Hyuk Kwon, Dae-Hyun Hwang
Korea Atomic Energy Research Institute, 111, Daedeok-daero 989Beon-gil, Yuseong-gu, Daejeon, Korea
**Corresponding author: juhyunglee@kaeri.re.kr*

Keywords : Soluble Boron-free SMR, KAERI Bundle CHF Database, MATRA-S Code, EPRI correlation, CHF LUT

1. Introduction

Light-water small modular reactors (SMRs), such as the i-SMR and LEU+ SMR currently under development in Korea, actively adopt a soluble boron-free (SBF) core concept to enhance reactor economics while simplifying chemical and operational systems. In SBF cores [1-3], soluble boron is not utilized for reactivity control; therefore, control rods (CRs) are required to provide relatively higher worth. The use of high-worth CRs can potentially introduce excess reactivity and may lead to increased local power peaking or local power distortion. To mitigate these effects, SBF cores typically incorporate additional CRs or fuel assemblies (FAs) containing numerous burnable absorbers (BAs), such as gadolinia (Gd_2O_3). From a thermal-hydraulic (T/H) perspective, these CRs and BA rods generate lower heat than fuel rods, thereby inducing a cold-wall effect which results in local coolant enthalpy depression in adjacent subchannels. Meanwhile, in SBF cores, the axial location of the peak power generally shifts upward with burnup. In particular, at the Beginning of Cycle (BOC), a bottom-peaked axial power distribution may be observed due to the rod-dominated reactivity control strategy. Accordingly, not only the presence of numerous non-heated rods (NHRs) but also the bottom-peaked axial power shape (APS) should be carefully considered as key characteristics of SBF reactors.

This study investigates the influence of nuclear design characteristics specific to SBF cores—such as multiple NHRs and bottom-peaked APSs—on the critical heat flux (CHF) from a general T/H perspective, since CHF plays a major role in the evaluation of core thermal margin. The Korea Atomic Energy Research Institute (KAERI) has established a bundle CHF database over several decades based on both open literature and proprietary data [4]. The database consists of CHF data obtained from various square and non-square test bundles. Because it covers a wide range of bundle geometries, mixing vane configurations and arrangements, as well as radial and axial power distributions, it enables the assessment of the effects of multiple NHRs and bottom-peaked APS from a CHF data perspective. In core design, it is essential to ensure that such SBF-related characteristics are adequately reflected in predictive models and do not adversely influence the minimum departure from nucleate boiling ratio (MDNBR) prediction. Therefore, a reference model was selected and applied to the database to evaluate its applicability to SBF core conditions. Accordingly, representative bundle CHF prediction approaches—the EPRI correlation and the Lookup Table (LUT) method with bundle correction factors—were implemented in the subchannel code MATRA-S developed by KAERI [8], and the present study was conducted based on these methodologies.

2. KAERI Bundle CHF Database

To investigate the CHF characteristics of light-water reactor cores, a total of 14,028 CHF data points from 251 test bundles were collected and compiled at KAERI. Among these, 8,207 data points were obtained from open literature, corresponding to 173 test bundles. The KAERI bundle CHF database includes test assemblies with a square-lattice rod arrangement as well as assemblies with various barrel geometries. The outer channel configurations include square, cruciform, circular, hexagonal, and rhombic shapes. The database covers a wide range of test configurations, from bundles without NHRs to those containing up to four NHRs ($N_{nh} = 0 \sim 4$). The dataset includes not only non-heated rods with diameters comparable to heated rods, but also large non-heated rods equivalent in size to approximately four heated rods, thereby enabling systematic assessment of cold-wall effects under different assembly geometric conditions. In addition, the database contains CHF data obtained under various axial power distributions, such as uniform, center-peaked, top-peaked, and bottom-peaked shapes, allowing evaluation of APS effects. For radial power distributions, the rod peak factor (F_r) ranges from 1.0 to 1.6, covering typical design conditions.

Detailed information on the test assembly configurations and CHF test ranges is provided in Ref. [4]. In this study, the database was utilized as extensively as possible, and the analysis was performed from a broad perspective to ensure a comprehensive assessment.

2. Model and Method

2.1 EPRI-1 Correlation

The EPRI correlation is a generalized bundle CHF correlation developed based on approximately 11,000 bundle test data obtained from the HTRF at Columbia

University. Detailed information on the correlation is available in Ref. [5] and is therefore omitted here.

In this study, a baseline model was implemented in the MATRA-S code to evaluate bundle CHF prediction performance. In this model, neither the cold-wall correction factor nor the grid spacer correction factor was applied; only the axial power distribution correction factor (C_{NU}) was considered in evaluating CHF based on subchannel properties calculated by MATRA-S code.

As reported in the original document, a total of 3,607 CHF data points were used to optimize the coefficients of the EPRI correlation, yielding a mean CHF P/M of 0.995 with a standard deviation of 7.2%. The KAERI bundle database contains 7,672 CHF data points derived from EPRI CHF database. Therefore, acceptable predictive performance was anticipated for this portion of the KAERI database.

2.2 CHF Lookup Table with Bundle Correction Factors

The CHF prediction capability for the KAERI bundle CHF database was evaluated using the MATRA-S code with the Groeneveld CHF LUT [6]. Groeneveld proposed bundle and grid spacer correction factors (K_2 and K_3, respectively) to extend the CHF LUT to bundle conditions [7]. Since CHF was predicted in this study using a subchannel analysis code, the bundle correction factor, K_2 was excluded. In addition, a pressure correction factor (K_P) was proposed to account for the pressure effect on bundle CHF. The bundle CHF was finally predicted from the 1995 CHF LUT as follows:

$$q''_{CHF} = LUT_{D_e=8mm} \times K_1 \times K_3 \times K_4 \times K_5 \times K_p \qquad (2.1)$$

where the applied correction factors are summarized in Table I.

CHF prediction performance was evaluated using the heat balance method (HBM), in which the power is iteratively adjusted until the predicted CHF coincides with the local heat flux at the corresponding location. In general, the HBM is known to provide improved predictive performance compared to the direct substitution method (DSM), in which the CHF LUT is directly applied. However, since the HBM requires iterative power calculations and consequently increases computational cost, the MATRA-S code was modified to incorporate an isolated channel concept in the heat balance calculation. During the power iteration process, it was assumed that the ratio of enthalpy rise in the open channel to that in the closed channel remains constant. That is,

$$\frac{X - X_{in}}{X_{iso} - X_{in}} = Const. \qquad (2.2)$$

Table I: Applied bundle CHF correction factors

Item	Parameter
Diameter [3]	$K_1 = \left(\frac{0.008}{D_e}\right)^{1/2}$ for $0.002 < D_e < 0.025$ $K_1 = 2.0$ for $D_e \le 0.002$ $K_1 = 0.566$ for $D_e \ge 0.025$
Grid spacer [3]	$K_3 = 1 + 1.5K_{grid}^{0.5}\left(\frac{G}{1000}\right)^{0.2} \exp\left(-0.1 \times \frac{L_{sp}}{D_e}\right)$
Heated length [3]	$K_4 = 1.0$ for $L/D_e \le 5$ $K_4 = \exp(e^{2\alpha} D_e/L)$ for $L/D_e > 5$ $\alpha = x_e/\left[x_e + (1 - x_e)\rho_g/\rho_f\right]$ for $x_e \ge 0.0$ $K_4 = 1.0$ for $x_e < 0.0$
Axial power shape [3]	$K_5 = 1$ for $x_e \le 0.0$ $K_5 = \frac{q''_{loc}(z_c)}{q''_{BLA}(z_c)}$ for $x_e > 0.0$ $q''_{BLA}(z_c) = \frac{1}{L_B}\int_{z_{x=0}}^{z_c} q''(z)dz$
Pressure (this study)	$K_P = 0.95 \times \left(0.884 + 0.18 \times (P/P_c)\right)$ for $P \ge 100$ bar $K_P = 0.95 \times \left(0.4 + 1.25 \times (P/P_c)\right)$ for $P < 100$ bar $P_c = 221.15$ bar

2.3 MATRA-S Model

The MATRA-S code (V1.2m0) is a subchannel analysis code for core T/H design developed by KAERI. The major model input parameters used in the subchannel analysis of the test bundles to assess the prediction capability against the KAERI CHF bundle database are listed in Table II. It should be noted here that the single-phase turbulent mixing parameter (TMP), also referred to as the turbulent diffusion coefficient (TDC), which governs turbulent mixing between adjacent subchannels, was not reported in most of the literature. In such cases, the TDC was assumed to be 0.005.

Local T/H properties at the MDNBR location were extracted from the MATRA output files using a Python script in order to investigate the effects of parameters such as geometric dimensions, local flow properties and power distributions on CHF prediction.

Table II: Involved MATRA-S subchannel parameters

Parameter	Value
Subcooled boiling void fraction	Not used
Bulk boiling void fraction	Chexal-Lellouche Model
Two-phase friction multiplier	Armand Model
Single-phase turbulent friction factor	$f = 0.184 \times \mathrm{Re}^{-0.2}$
Crossflow resistance coefficient	$K_{ij} = 0.5$
Lateral momentum parameter	$s/l = 0.5$
Turbulent momentum factor	$f_T = 0.0$
Turbulent mixing model	Equal-mass-exchange
Turbulent mixing parameter	$\beta = 0.005 \sim 0.062$
Void drift	Not used
Solution algorithm	Implicit scheme

3. Results and Discussion

3.1 Overall Performance

Fig. 1 presents the evaluation results of the KAERI bundle CHF database obtained using the MATRA-S code with the EPRI correlation and the LUT HBM. The results are expressed in terms of CHF P/M versus local mass flux at the MDNBR location. As shown in the figure, both the EPRI correlation and the LUT HBM demonstrate acceptable predictive performance. The mean and standard deviation of CHF P/M are 0.942 and 0.110 for the EPRI correlation, and 0.940 and 0.110 for the LUT HBM, respectively, which indicates comparable prediction capability. However, the EPRI correlation tends to underpredict CHF in the low mass flux region (G < ~1,000 kg/m²-s). In contrast, for the LUT HBM, the predicted CHF under uniform axial power distribution conditions is higher than that under non-uniform axial power distributions in some cases.

Overall, since the database includes a large number of data covering various bundle geometries and operating conditions, the results confirm that both models are suitable as reference model and correlation for general design applications.

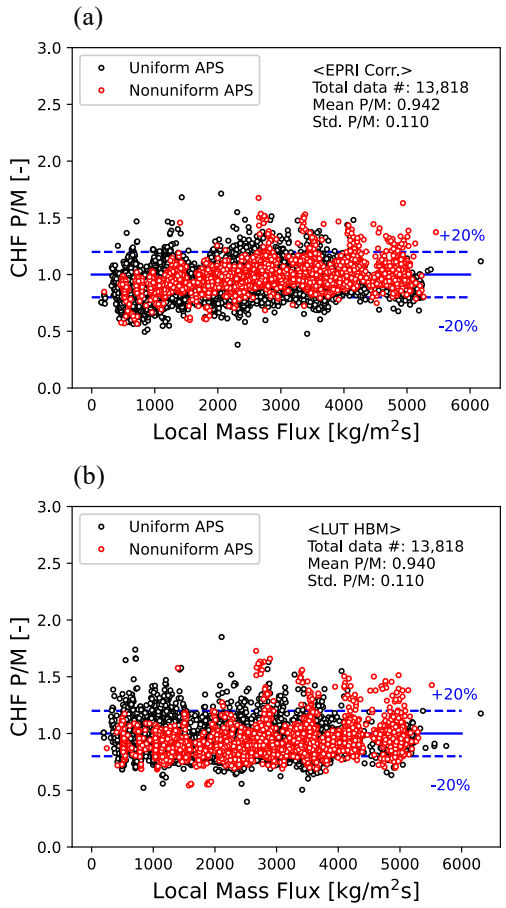

Fig. 1. CHF P/M vs Local Mass Flux based on (a) EPRI-1 correlation (b) LUT HBM

It should be noted that approximately 180 cases (about 1.3% of the total KAERI bundle CHF database) were excluded from the present evaluation due to computational errors in the MATRA-S calculations. In addition, for the EPRI-35 dataset obtained under uniformly heated 5×5 square bundle tests, most of the data (approximately 70%) were beyond $\mu + 2\sigma$; therefore, this dataset (26 data points) was excluded from the analysis. Consequently, a total of 13,818 CHF data points were used in the final evaluation of CHF prediction performance in this study.

3.2 Effect of SBF-core-related Parameters

To evaluate the effects of non-heated rod configuration and bottom-peaked APS conditions associated with the SBF core design on MDNBR prediction performance, the KAERI bundle CHF database was regrouped as summarized in Table III. The prediction performance was re-evaluated accordingly.

Table III: Data Grouping for analysis

Non-heated rod		**APS**	
Large	3,436	Bottom (AO=-0.482~-0.218)	236
N_{nh}=0	6,212	Center (AO=-0.002~+0.055)	1,184
N_{nh}=1	2,694	Top (AO=+0.165~+0.482)	1,233
N_{nh}>1	1,476	Uniform	11,165
Total	13,818	Total	13,818

Figs. 2 and 3 present the results grouped by non-heated rod configuration and axial power peak location, respectively. For each group, the mean CHF P/M is shown with ±2σ error bars. The results for the EPRI correlation and LUT HBM are presented in Figs. 2 and 3, respectively.

For the EPRI correlation (Fig. 2(a)), CHF P/M slightly increases in bundles with multiple NHRs ($N_{nh} > 1$) compared to cases with one or no NHRs. However, the increase is limited to approximately 6–7%, which is not significant considering the group standard deviation of ~11%. For bundles with a large single NHR equivalent in size to multiple heated rods, CHF P/M is comparable to that for smaller NHRs, while the standard deviation decreases to approximately 9%, indicating slightly improved prediction performance. Overall, the variation in prediction performance due to NHR configuration is minor when the EPRI correlation is used with MATRA-S. Regarding APS effects, bottom-peaked conditions result in approximately 10% lower CHF P/M compared to top-peaked conditions. From a design perspective, lower P/M results in conservative CHF prediction and therefore enables conservative SBF thermal margin evaluation. The standard deviation remains

approximately 11% across bottom-, center-, top-skewed peak, and uniform APS conditions.

Fig. 3 summarizes the effects of major parameters on the prediction performance of the LUT HBM. Regarding NHR configuration (Fig. 3(a)), CHF P/M increases by approximately 5–7% in groups with multiple NHRs, similar to the trend observed for the EPRI correlation. The standard deviation remains within 10–11% across different NHR configurations. However, the effect of a large single NHR is more noticeable in the LUT HBM than in the EPRI correlation. In cases with a large NHR, CHF P/M decreases to approximately 0.91, indicating increased dependence on this configuration. This suggests that the LUT HBM could be further improved to better account for large NHR effects. For APS effects (Fig. 3(b)), the LUT HBM exhibits consistent prediction performance regardless of axial peak location. Compared with the EPRI correlation results in Fig. 2(b), the tendency to overpredict under top-peaked conditions and underpredict under bottom-peaked conditions are substantially reduced. However, the standard deviation increases by approximately 6–30% relative to the EPRI correlation.

3. Conclusions

From the perspective of SBF core design incorporating multiple NHRs and bottom-peaked APS conditions, the MDNBR prediction performance of the EPRI correlation and LUT HBM was evaluated using MATRA-S. The evaluation was based on the KAERI bundle CHF database, which covers a wide range of bundle geometries, axial power distributions, and operating conditions, enabling a generalized assessment of model performance. The results indicate that both models, when applied with MATRA-S, reasonably predict MDNBR while reflecting the effects of NHR configuration and APS. However, in the detailed design stage, CHF correlations should be developed using separate effect test data obtained from test bundles that reflect specific core features (such as grid geometry and arrangement), and used for final thermal margin evaluation. Therefore, the DNB evaluation methodology described in this study can serve as a reference model for thermal margin assessment in the conceptual design of SBF reactors.

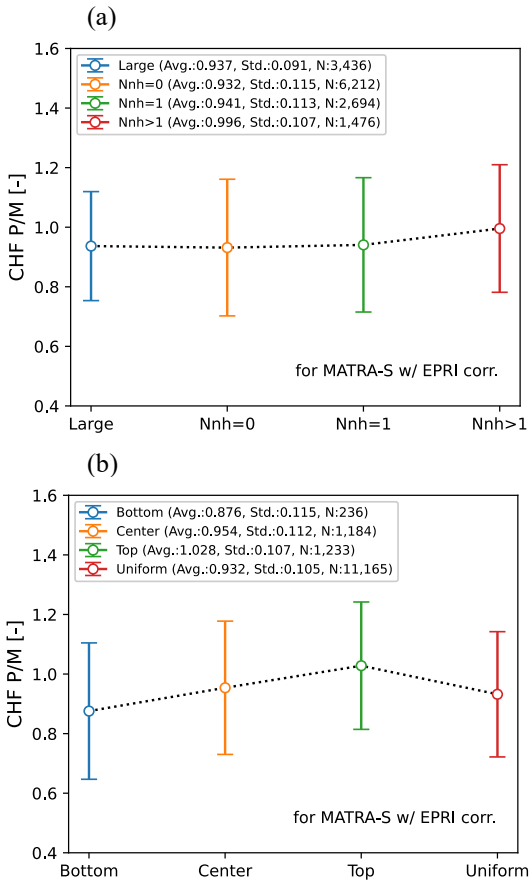

Fig. 2. Effect of SBF related parameters – EPRI correlation: (a) Non-heater rods (b) Axial power shape

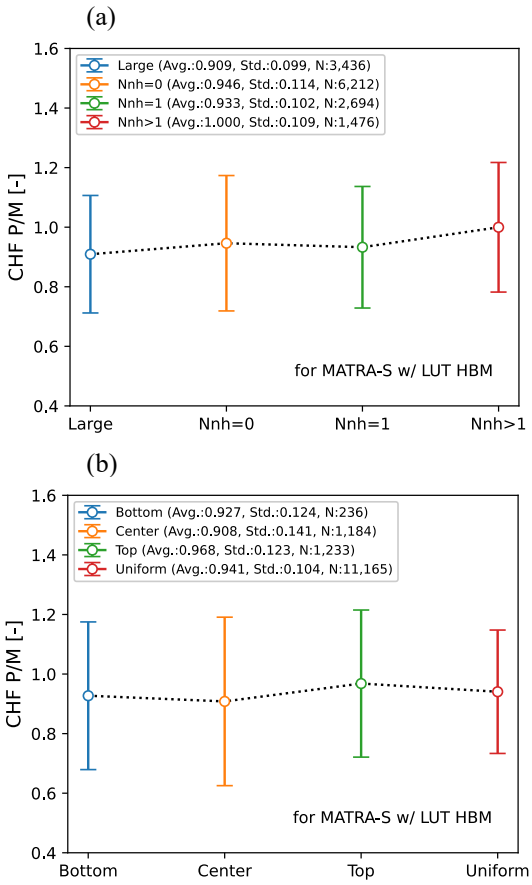

Fig. 3. Effect of SBF related parameters – LUT HBM: (a) Non-heater rods (b) Axial power shape

ACKNOWLEDGMENTS

This paper was supported by the Innovative Small Modular Reactor Development Agency grant funded by the Korea Government(MSIT R&D) (NO. RS-2023-00258205).

REFERENCES

[1] X. H. Nguyen et al., An advanced core design for a soluble-boron-free small modular reactor ATOM with centrally-shielded burnable absorber, Nucl. Eng. Technol. 51, p.369-376 (2019)

[2] J. S. Kim et al., Reactor core design with practical gadolinia burnable absorbers for soluble boron-free operation in the innovative SMR, Nucl. Eng. Technol. 56, p.3144-3154 (2024)

[3] C. Lee et al., Full-core fuel analysis of a soluble boron-free SMR: Pellet-cladding interaction issue and enhancing fuel safety through loading pattern design, Nucl. Eng. Technol. 57, 103709 (2025)

[4] D. H. Hwang et al., Compilation of Rod Bundle CHF Data Base for LWR Cores, KAERI/TR-11119/2025, KAERI (2025)

[5] D. G. Reddy and C. F. Fighetti, Parametric Study of CHF Data Volume 2: A Generalized Subchannel CHF Correlation for PWR and BWR Fuel Assemblies, EPRI-NP-2609, Vol.2 (1983)

[6] D. C. Groeneveld, The 1995 look-up table for critical heat flux in tubes, Nucl. Eng. Des. 163, p.1-23 (1996)

[7] D. C. Groeneveld et al., Lookup Tables for Predicting CHF and Film-Boiling Heat Transfer: Past, Present, and Future, Nucl. Tech. 151, p.87-104 (2005)

[8] H. Kwon et al., Validation of a Subchannel Analysis Code MATRA version 1.1, KAERI/TR-5581/2014, KAERI (2014)